Infrared Spectroscopic Ellipsometry of *n*-Alkylthiol (C_5-C_{18}) Self-Assembled Monolayers on Gold

Z. G. Hu, P. Prunici, P. Patzner, and P. Hess*

Institute of Physical Chemistry, University of Heidelberg, Im Neuenheimer Feld 253, D-69120 Heidelberg, Germany

Received: January 27, 2006; In Final Form: May 9, 2006

The infrared spectroscopic ellipsometry (IRSE) of *n*-alkylthiol ($CH_3(CH_2)_xSH$, $x = 4$, 6, 7, 8, 10, 13, 15, and 17, self-assembled monolayers (SAMs), with 5−18 carbon atoms (C_5−C_{18}), grown on gold-coated Si(100) substrates) was investigated at room temperature. The C−H stretching vibrations could be resolved even for pentathiol, the shortest chain studied. The symmetric and asymmetric stretching vibrations of the CH_2 groups are located at about 2850 and 2920 cm^{-1}, and those of CH_3 are at about 2877 and 2962 cm^{-1}, respectively; they show a slight shift with the number of CH_2 units. In addition, Fermi resonance of the symmetric CH_3 stretching vibration at 2940 cm^{-1} appears with decreasing chain length due to weak coupling with the asymmetric CH_2 stretching vibration. The "odd−even effect" of the *n*-alkylthiol SAMs with varying CH_2 units could be distinguished by the two interactive IRSE parameters. The relative ellipsometric spectra for the four longest chains could be reproduced quite well by using a Lorentz multioscillator model with a three-phase optical model (air/SAMs/gold). On the basis of the theoretical calculations, the vibrational strength of these oscillators is very weak, its magnitude being 10^{-4}−10^{-5}. The full width at half-maximum (fwhm) of the peaks varies from 7 to 33 cm^{-1}. Moreover, the intensity of the C−H vibrations increases with the number of methylene units, due to strong lateral interactions and ordering effects occurring for longer chains.

1. Introduction

The formation of self-assembled monolayers (SAMs) of *n*-alkylthiols ($CH_3(CH_2)_xSH$) on gold films has attracted intensive attention in many fields, such as catalysis, wetting, sensing, and molecular electronics.[1−3] The kinetics of SAM formation, where the final equilibrium state is controlled by the packing density and the interaction between tails and the configuration of the headgroups (e.g., CH_3), has been investigated for several years.[4−6] Some unique features of SAMs have been studied with use of optical techniques, such as Fourier transform infrared reflection−absorption spectroscopy (FT-IRRAS) and attenuated total reflection (ATR), which can be applied to characterize the composition and molecular structure of SAMs on noble metal surfaces.[1,7−10] In principle, four vibration frequencies can be resolved in the infrared spectra of *n*-alkylthiols, the d^+ and d^- modes, which are ascribed to the symmetric and asymmetric CH_2 stretching vibrations, and the r^+ and r^- modes, which represent the symmetric and asymmetric CH_3 stretching vibrations, respectively.[11] The actual C−H vibrations of SAMs depend on the immersion time, solvent concentration, temperature during preparation, and metal substrate.[1,6] Normally the oscillator strength of CH_2 and CH_3 vibrations increases with the chain length and the corresponding structural rearrangement.[11] It should be noted that previous reports mainly focused on SAMs with long chains (i.e., $x \geq 8$), using infrared spectroscopy.[6,8,10,11] Fermi resonance of the symmetric CH_3 stretch r_{FR}^+ was observed at 2938 cm^{-1} for C_6−C_{22} *n*-alkylthiol SAMs on platinum films.[1] Bryant and Pemberton reported on surface Raman spectroscopy of C_4−C_{18} *n*-alkylthiol SAMs on rough gold films.[12] They found that the frequencies of the symmetric vibrations are more intense in the long-chain *n*-alkylthiols. However, detailed information on *n*-alkylthiol SAMs with a small number of methylene units is still scarce.

Although FT-IRRAS measurements are sensitive to the number of CH_2 units and ordering effects, some subtle structures, such as shoulders on particular peaks, are difficult to detect and to assign.[6] Small changes in spectral reflection can result in unexpected peak broadening and intensity variations because of artificial baseline corrections.[13] Fortunately, these problems can be recognized with spectroscopic ellipsometry and weaker molecular vibrations can be identified unambiguously with the Kramers−Kronig transformation (KKT).[14−16] In particular, the KKT presents specific pairs of vibrational features and makes it easier to assign the vibrational modes. Just recently, infrared spectroscopic ellipsometry (IRSE) has been used to characterize SAMs and ultrathin films on metals and semiconductor substrates.[16−20] In general, chemical bonds such as C−H have different orientations, which may be oblique to the substrate surface.[11] IRSE measures the change of the amplitude and phase for p- and s-polarized light reflected from the samples, whereas in FT-IRRAS and ATR spectroscopy usually unpolarized light is used. IRSE is a surface-sensitive tool and extends the detection limit to the atomic scale for well-defined isotropic layers. However, unlike ATR spectroscopy, which collects multiple reflections in a transparent crystal such as single-crystal silicon, IRSE measures single reflection signals and uniquely distinguishes the weaker vibrations by two synchronously recorded ellipsometric parameters.

Meuse reported that with IRSE the signals of hexadecanethiol (C_{16}) and dodecanethiol (C_{12}) SAMs on gold films could be detected but not those of hexanethiol (C_6).[17] Bradford et al. studied the vibrational properties of octadecylmercaptan, undecanethiol (C_{11}), and dodecanethiol (C_{12}) SAMs on nanoislands

* Address correspondence to this author. E-mail: peter.hess@urz.uni-heidelberg.de.

10.1021/jp060596y CCC: $33.50
Published on Web 07/11/2006

and flat gold surfaces by the IRSE method.[18,21] They found that the surface morphology of the gold film can strongly affect the signal intensity and a signal enhancement of about 40 was found for the nanoisland films. Nevertheless, the r_{FR}^{+} vibration (Fermi resonance) could not be resolved.[21] Note that the incident angle was about 70°, which is far from the Brewster angle of gold.[19,22] Unlike the lattice vibrations of semiconductor films, the C−H stretches are so weak that the analysis is very sensitive to the incident angle in experiments with polarized light.[9,11,23,24] Thus, it is important to select the optimal angle of incidence in such IRSE experiments. To our knowledge, no studies have been presented for *n*-alkylthiol SAMs with varying CH_2 units using the IRSE technique except for Meuse's report.[17]

In this article, the C−H vibrations of C_5−C_{18} SAMs deposited on gold films are investigated on the basis of IRSE spectra. The sensitivity needed to detect these bands in C_5 SAMs could be achieved. In particular, the effects generated by varying the number of CH_2 units on the vibrational frequencies, line strength, and line broadening are studied in detail. A theoretical simulation based on the Lorentz oscillator model is presented to model the IRSE data.

2. Experimental Section

Deposition of Gold Films and SAMs. Gold films were deposited on Si(100) wafers by evaporation in a vacuum chamber (1×10^{-5} Torr). A titanium layer with a thickness of 2−4 nm was first deposited on the silicon substrate to improve the adhesion of the gold film. Then continuous gold films with a nominal thickness of 30 and 100 nm were deposited. The thickness of the films was controlled with a quartz-crystal microbalance. All gold films were cleaned with an ultraviolet (UV) lamp and ethanol before the deposition of SAMs. Thorough cleaning or oxidizing SAMs on gold surfaces for a longer time could affect the metallic film and may result in a gold-oxide layer, which can decrease the sensitivity.[1,25] Therefore, the oxidation time was limited to 1−3 min. Two different preparation methods are commonly employed, namely, deposition either from solution or from the gas phase.[4,5,26] In this work, the C_5−C_{18} SAMs were prepared from solution. The octadecanethiol (98%), hexadecanethiol (95%), tetradecanethiol (98%), undecanethiol (98%), nonethiol (95%), octathiol (98.5%), heptanethiol (95%), and pentathiol (98%) *n*-alkylthiol samples were obtained from Aldrich and used as received. The SAMs were prepared by immersing the gold films into ethanol solutions with a concentration of 1 mM. Ethanol was used as the solvent because it dissolves most *n*-alkylthiols and can be readily obtained in pure form. All immersion experiments were performed at room temperature.

After the growth process the samples were rigorously cleaned in pure ethanol with an ultrasonic bath to remove physisorbed molecules from the SAM surface. Finally the SAMs were dried in a pure nitrogen stream. Then the IRSE measurements were performed immediately. The *n*-alkylthiol SAMs with longer chains were found to be intact after several weeks of exposure to air while the samples with shorter chains were deteriorated.[11,27,28] Saturation of SAM coverage as a function of immersion time could be probed by IRSE, by detecting the intensity of the CH_2 and/or CH_3 vibrations. These signals will not change after optimal preparation.[29] For the C_{18} SAMs, the optimal immersion time was 1.5 h. For the SAMs with shorter chains, the immersion time was increased up to 3 h.[6,27] Even for substantially longer preparation times (e.g., 2 days for the C_5 SAMs) no evident variations could be seen in the IRSE spectra. In addition, FT-IRRAS spectra with *p*-polarized light incident at an angle of 80° were acquired to further characterize the SAM formation process. These spectra showed a similar structure as described previously. This indicates that the SAMs were highly oriented and ordered.[1,11]

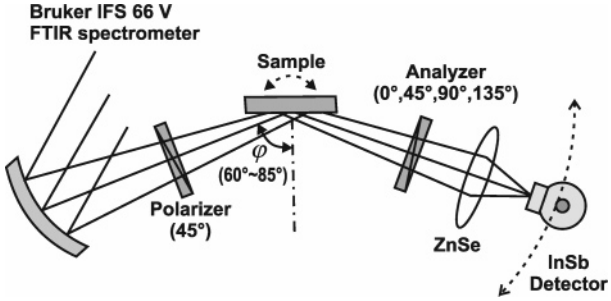

Figure 1. Scheme of the experimental setup used for IR spectroscopic ellipsometry.

The surface morphology of the gold films was analyzed by atomic force microscopy (AFM) (Digital Instruments Dimension 3100, Veeco Instruments). The roughness of the gold films was characterized with the tapping mode in areas of $5 \times 5\ \mu m^2$. For gold films with thicknesses of 30 and 100 nm, the root-mean-square roughness was about 0.7 and 1.5 nm, respectively. No evident differences in the IRSE spectra could be noticed for these substrates. Therefore, the IRSE data obtained for the *n*-alkylthiol SAMs on the 100-nm-thick gold films will be selected for the following discussion.

IRSE Measurements. Mid-IR (MIR) ellipsometric spectra of the *n*-alkylthiol SAMs were measured with a Bruker IFS 66V Fourier transform infrared (FTIR) spectrometer. In addition to the FTIR spectrometer, the instrument consisted of flat and elliptical gold mirrors, a polarizer, sample table, analyzer, and detector (see Figure 1).[17,30] The gold mirrors were used to make the IR beam parallel and to focus it onto the sample. The polarizer was a KBr wire grid KRS-5 polarizer (Optometrics LLC) and was oriented 45° to the incident plane. The sample table and detector arm were driven by two stepping motors (Model C-161.2i, Physik Instrumente GmbH, Germany). The analyzer and rotation accessory (Bruker Optics Inc.) were fixed to each other and turned together with the detector arm.

IRSE spectra of the C_{18} SAMs were first studied at different incident angles to determine the angle dependence. Then all experimental data were recorded at an angle of incidence of 83 ± 2°, optimized for the gold substrate. A liquid nitrogen cooled InSb detector and optimized KBr beam splitter were used for detection with a spectral resolution of 4 cm^{-1}. In the wavenumber region of the C−H stretching vibrations (2700−3000 cm^{-1}), the sensitivity of the InSb detector is much higher than that of the MCT detector, usually used in the MIR region. In particular, it is preferable to measure the small reflection intensity from the SAM surface by rotating the analyzer due to the high absorption index of the gold substrate.[22] Note that a ZnSe convex lens was employed to focus the light onto the sensitive detector element, whose polarization effects were not taken into account.

To obtain the ellipsometric parameters, four analyzer positions (0°, 45°, 90°, and 135°) were automatically collected, using the OPUS macro language of the Bruker FTIR spectrometer. The collection time for each analyzer position was extended to 10 min to reduce the contributions from water and CO_2 in the

ambient atmosphere. Thus, the ellipsometric parameters Ψ and Δ can be readily obtained from[16,30]

$$\cos 2\Psi = \frac{I(90°) - I(0°)}{I(90°) + I(0°)}$$

$$\sin 2\Psi \cos\Delta = \frac{I(45°) - I(135°)}{I(45°) + I(135°)} \quad (1)$$

Here, I refers to the measured light intensity at the corresponding azimuthal angles of the analyzer. For each set of four scans the above FTIR parameters were kept fixed. The samples were kept at room temperature and no mathematical smoothing of the experimental data was performed. The ellipsometric data of the gold films were measured separately and used as reference spectra in the spectroscopic analysis. It should be emphasized that the second part of eq 1 is used to determine the Δ values, which are less accurate than the Ψ ones. This is due to the fact that there is very little light on the detector when the polarizer and analyzer are crossed (i.e., the analyzer position is 135°). Therefore, the scanning experiments were repeated many times to estimate the errors involved. The observed deviations were within the 1.0% and 2.5% limits for the Ψ and Δ values, respectively. It is important to compare these data with gold reference spectra due to the drawbacks of wire grid polarizers and infrared beam broadening in the optical path.[17]

3. Results and Discussion

Theoretical Background. Spectroscopic ellipsometry (SE), based on the reflectance configuration, deals with the measurement of the relative changes in the amplitude and phase of linearly polarized incident light upon oblique reflection from a sample surface.[14] The experimental SE parameters are the angles Ψ and Δ, which are related to the optical and structural properties of the sample, defined by

$$\rho \equiv \frac{\tilde{r}_p}{\tilde{r}_s} = \tan\Psi \exp(i\Delta) \quad (2)$$

Here, $\tilde{r}_p$ and $\tilde{r}_s$ are the complex reflectance coefficients of polarized light parallel and perpendicular to the plane of incidence, respectively. The complex reflectance coefficients of a single film on a substrate can be calculated by Snell's law if the film is isotropic.[31] The 2×2 matrix method is used to calculate the ellipsometric parameters of a SAM on a gold film since it enables easy calculation of the reflection for isotropic layers under oblique incidence. Suppose the complex dielectric function of a SAM is $\tilde{\epsilon}_f$, unity for vacuum, and $\tilde{\epsilon}_s$ for the substrate. The resultant matrix M_r is then described by the following expression:[31,32]

$$M_r = M_{01} M_1 M_{12} \quad (3)$$

Here, $M_{j,j+1}$ is the interface matrix

$$M_{j,j+1} = \frac{1}{\tilde{t}_{j,j+1}} \begin{bmatrix} 1 & \tilde{r}_{j,j+1} \\ \tilde{r}_{j,j+1} & 1 \end{bmatrix} \quad (4)$$

$\tilde{t}_{j,j+1}$ and $\tilde{r}_{j,j+1}$ are the transmittance and reflectance coefficients, respectively, which have different expressions for the p- and s-polarized reflected light.[31] M_1 is the propagation matrix for the SAMs layer

$$M_1 = \begin{bmatrix} \exp(i2\pi t\sqrt{\tilde{\epsilon}_f}\cos\varphi/\lambda) & 0 \\ 0 & \exp(-i2\pi t\sqrt{\tilde{\epsilon}_f}\cos\varphi/\lambda) \end{bmatrix} \quad (5)$$

where λ is the incident wavelength, t is the SAMs thickness, and φ is the angle of refraction. Thus, the total reflectance coefficients $\tilde{r}_p$ and $\tilde{r}_s$ can be calculated from

$$\tilde{r}_{p,s} = \frac{M_{r2,1}}{M_{r2,2}} \quad (6)$$

The C−H vibrations can be described by the harmonic Lorentz oscillator model, in which the dielectric function is defined as a response function with four pairs of poles. Accordingly, the dielectric function of the *n*-alkylthiol SAMs can be written as

$$\tilde{\epsilon}_f = \epsilon_\infty + \sum_{j=1}^{4} \frac{S_j \omega^2_{CH,j}}{\omega^2_{CH,j} - \omega^2 - i\omega\gamma_j} \quad (7)$$

Here, ϵ_∞, $\omega_{CH,j}$, S_j, and γ_j represent, in order, the high-frequency dielectric constant, the C−H stretching center angular frequency, the strength of the stretching vibration, and the full width at half-maximum (fwhm) of the absorption peak. Correspondingly, the optical constants ($\tilde{n} = n + i\kappa$) are calculated from the relationship $\tilde{n} = \sqrt{\tilde{\epsilon}_f}$. Here, n is the refractive index and κ is the absorption index or extinction coefficient.

It should be emphasized that an anisotropic dielectric function model, such as the optical tensor construction, which considers a surface-bound all-trans SAM chain with tilt, twist, and azimuth angles, would be needed to completely describe the infrared spectral responses.[33] Such calculations are based on a 4×4 matrix method and become very complicated because of the so-called p- and s-mode coupling.[33,34] However, the p- and s-modes are mutually orthogonal and uncoupled in isotropic media, where the 2×2 matrix calculation is sufficient. Hoffmann et al. assumed a uniaxial symmetry around the surface normal for the SAM layer to separate the p- and s-polarization calculations based on the 2×2 method.[13,35] An ellipsometric analysis, which accounts for polarization mixing at interfaces, should be more sensitive to extract the anisotropic structure of SAMs.[34] As Parikh and Allara stated, each vector of the anisotropic function model can be constructed by using the isotropic optical constants of the reference samples.[33] Moreover, many vibrational absorption bands of chemical surface entities can be modeled satisfactorily by assuming a Lorentz oscillation, which reveals the individual oscillator parameters.[30]

The parameter values in eq 7 can be found by applying a Levenberg−Marquardt algorithm, which is an efficient nonlinear calculation method for many-parameter fitting.[36] The dielectric function $\tilde{\epsilon}_s$ of the gold film, used in the calculations, was measured by using IRSE and shows slight deviations from bulk gold samples.[37] This may be due to a different film density and structure.[21] It should be emphasized that only the amplitude variation $\tan\Psi$ was taken into account in the present calculations. The comparability of $\tan\Psi$ spectra of SAMs or ultrathin organic films on metallic substrates and standard transmission spectra originates from the so-called "surface selection rule", which is due to the small difference of the s-polarized reflectance coefficients $\tilde{r}_s$ between the SAMs and the gold reference

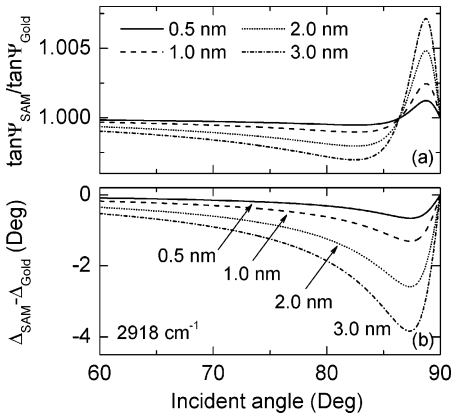

Figure 2. The dependence of the real part (a) and imaginary part (b) of the relative complex optical density of SAMs with different thicknesses on the incident angle for the asymmetric CH_2 vibration at 2918 cm^{-1}. The optical constants of the SAMs were taken as $\tilde{n}_f = 1.5 + i0.1$ [ref 9] and those of the gold film were derived from the present IRSE measurements ($\tilde{n}_s = 3.3 + i21.8$).

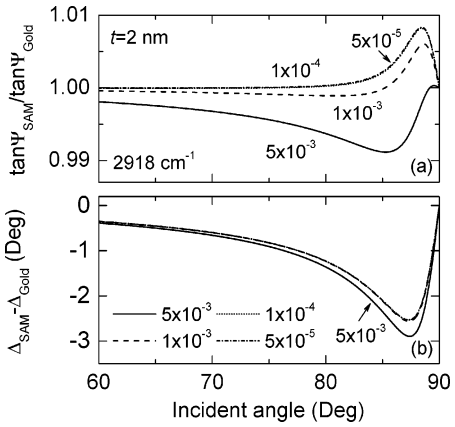

Figure 3. Dependence of the real part (a) and imaginary part (b) of the relative complex optical density for SAMs with different vibrational strengths on the incident angle for the asymmetric CH_2 mode. A thickness of 2 nm was assumed and the refractive index n of the SAMs was kept at 1.5, which means that the absorption index κ increases from 0.003 to 0.3 with the strength S varying from 5×10^{-5} to 5×10^{-3}. The broadening γ is set to 15 cm^{-1} in eq 7. The changes for the three smaller S values are too tiny to be seen in part b.

spectra.[22,38] However, it is difficult to accurately determine the Δ value near $\Delta = 0°$ and 180° with the rotating analyzer system used in the present experiments. The spectral dependence of Δ can help to uniquely assign the vibration bands by the KKT.[39]

Theoretical Studies on the Dependence of the Complex Optical Density on Incident Angles. IRSE is sensitive to the incident angle and can be performed near the Brewster angle of the substrate material.[14] This is due to a striking difference between the p- and s-polarized light reflected from the sample. However, the exact Brewster angle should be avoided because the p-polarized reflected light intensity approaches zero there. Furthermore, for the detection of weak vibrations, measurements near the surface normal fail to obtain the spectral information. The incident angle is a critical factor for SAM measurements due to the small film thickness on the order of a few nanometers. An incident angle of about 85° has been used in infrared polarized reflection experiments on *n*-alkylthiol SAMs on metal substrates.[11,22] On the other hand, the angle of incidence was 70° in recent IRSE measurements of SAMs or ultrathin films on gold substrates.[17,18,20,21] As stated by Tompkins at al., an optimized incident angle is required for a highly sensitive analysis of ultrathin films on gold substrates.[19] Therefore, a detailed simulation was performed to clarify the relationships between the ultrasmall thickness, weak vibration, and incident angle in an IRSE experiment.

Relative ellipsometric data based on a comparison with the gold reference data have been widely adopted in IRSE studies of SAMs due to the weak vibration bands of monolayers and the imperfect discrimination of polarized light by the polarizer and/or analyzer setup.[17,18] The quantity $\tan\Psi_{SAM}/\tan\Psi_{Gold}$ refers to the real part of the relative complex optical density while $\Delta_{SAM} - \Delta_{Gold}$ is the corresponding imaginary part of the relative complex optical density. The calculated dependence of the complex optical density on the incident angle is shown in Figure 2 for different layer thicknesses. The results for angles from 60° to 90° are plotted, spanning the range of typical ellipsometric measurements. The calculations were performed for the frequency of the asymmetric CH_2 stretching vibration at 2918 cm^{-1}. A similar behavior is expected for the other modes. Note that the real part of the complex optical density is unity at the incident angles of 0°, 86° (Brewster angle), and 90° while the imaginary part shows an asymmetric dip near the Brewster angle and approaches zero at the incident angles of 0° and 90°. The baseline deviations of the imaginary part from zero are ascribed to thickness contributions, which result in the phase shift of the p- and s-polarized light. This unique feature is lost in FT-IRRAS, which only records the reflected optical intensity information.

There is an opposite trend for the thickness variation below and beyond the Brewster angle, which depends on the optical constants of gold ($\tilde{n}_s = 3.3 + i21.8$). The relative value of the real and imaginary parts of the optical density decreases with decreasing film thickness below and above certain incident angles, which are located near the Brewster angle. This demonstrates that thicker films are easier to measure with the IRSE technique, as is true for other spectroscopic techniques. Although the difference of the Δ value between film sample and gold substrate is maximal at the Brewster angle, the real part $\tan\Psi$ cannot give any information on the sample (i.e., $\tan\Psi_{SAM}/\tan\Psi_{Gold} = 1$). Note that there is a minimum in the real part of the complex optical density near an incident angle of 83°, where the imaginary part still possesses a relatively large value. Thus, the angle should be optimized experimentally taking the tradeoff of the two measured ellipsometric parameters into account. As can be seen in Figure 2, the complex optical density at an incident angle of 70° is closer to the gold reference, i.e., the relative real part approaches unity and the relative imaginary part zero. Obviously, a larger angle is advantageous for resolving the vibrational bands of short end groups.

The reflected infrared light intensity depends not only on the thickness, but also on the particular oscillator strength. Figure 3 shows the effect of strength on the complex optical density for different incident angles. The strength was taken from fitting procedures and varies from 5×10^{-3} to 5×10^{-5} for the complex optical density. For strong vibrations, an angle strongly deviating from the Brewster angle can apparently be selected, which corresponds to the treatment of polar semiconductor films.[24,32] However, an angle near the Brewster angle is preferable for weak vibrational bands.[35] Note that the imaginary part exhibits much smaller variations at low oscillator strength than the thickness contribution. This explains the experimental observation that vibrations of short chains with weak vibrations (r_{FR}^+) did not appear at small incident angles.[17,18] It should also be noted that the calculated results are based on some simplifications, e.g., the anisotropic structure of the *n*-alkylthiol SAMs was not taken into account.[40,41] Nevertheless, the results

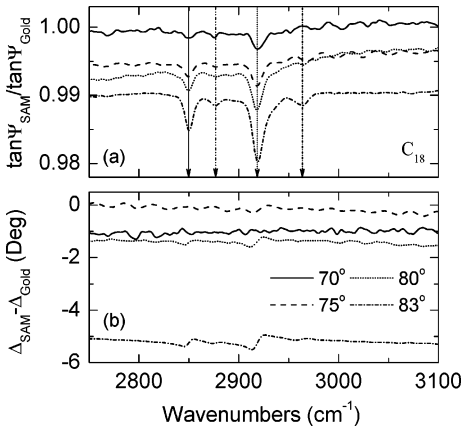

Figure 4. Relative complex optical density, (a) $\tan\Psi_{SAM}/\tan\Psi_{Gold}$ and (b) $\Delta_{SAM}-\Delta_{Gold}$, of the C_{18} SAM on gold films measured at different incident angles. The arrows indicate four typical C−H stretching vibrations.

provide a description of the variation of spectral signals with the incident angle and realize the optimized experimental configuration for the detection of weak vibrations.

As an experimental verification, the relative complex optical density of the C_{18} SAMs measured at different incident angles (70°, 75°, 80°, and 83°) is presented in Figure 4, demonstrating that the C−H absorption peaks strongly depend on the angle of incidence. At an incident angle of 70°, the symmetric and asymmetric CH_2 stretching vibration could be observed but the dips in Figure 4a are weaker than those measured at larger angles. The real part is closer to unity and the imaginary part approaches zero at smaller incident angles. Moreover, the derivative patterns of $\Delta_{SAM} - \Delta_{Gold}$ in Figure 4b can be clearly resolved only at angles beyond 80°. The reflection signal principally comes from the gold film and at smaller angles the "optical path length" in the SAMs (see eq 5) is shorter than that at larger angles. Therefore, the spectral information of the gold film dominates the IRSE spectra even for the SAMs with longer chains.

The optical throughput decreases rapidly with increasing angle of incidence due to the optical configuration and the spectral noise decreases with decreasing incident angle. However, the signal-to-noise ratios at these incident angles seem to be different and the deviation of the baseline of $\Delta_{SAM} - \Delta_{Gold}$ at the angle of 75° is minimal (see Figure 4). We assume that the perturbations of the optical path (such as a small misalignment) may contribute to these deviations.[42] In particular, artifacts and stray light are easily introduced at large angles of incidence because the optical paths of the SAM and gold reference are not the same and the infrared beam of the FTIR spectrometer is not strictly parallel. An optional method is to add an iris to obtain a better angle resolution and optical path alignment at the cost of decreasing light intensity. Note that the stronger C−H vibration signals reduce the influence of noise at larger angles of incidence, as shown in Figure 4. The present IRSE results clearly indicate that the optimal angle is near 83° for untrathin films on gold in polarized spectral experiments.[11,19]

IR Ellipsometric Spectra. The IRSE spectra Ψ and Δ of the C_5−C_{18} *n*-alkylthiol SAMs are shown in Figure 5, parts a and b, respectively. In all spectra, the asymmetric CH_2 (∼2920 cm^{-1}) and CH_3 (∼2962 cm^{-1}) stretching vibrations are observed, indicating the high sensitivity of IRSE compared with previous reports.[17,21] The arrows in Figure 5 indicate four typical C−H stretching vibrations, which can be assigned to the symmetric and asymmetric CH_2 and CH_3 modes. The CH_2

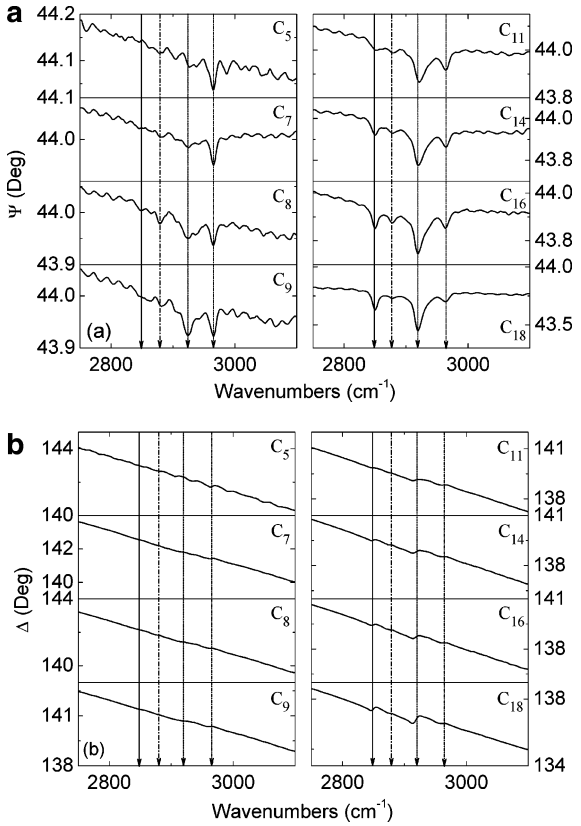

Figure 5. Experimental IR ellipsometric spectra, (a) Ψ and (b) Δ, of *n*-alkylthiol SAMs with varying CH_2 units on gold films. For clarity, the spectra are shifted vertically. The arrows indicate the four typical C−H stretching vibrations. Note that the asymmetric CH_3 stretching mode r^- could be observed at 2965 cm^{-1} even for the C_5 SAMs.

vibration intensity increases with the number of CH_2 units in longer chains. Although the gold films mainly contribute to the Δ spectra due to the "surface selection rule", the corresponding vibrational information also can be obtained at least for some SAMs. The derivative pattern in the Δ spectra obviously corresponds to the absorption-like bands in the Ψ spectra, which can be unambiguously ascribed to the C−H vibrations. As mentioned before, the spectral relationship between the two ellipsometric parameters is given by the KKT. Bradford et al. reported that the vibrational properties of C_{11} and C_{12} SAMs on flat gold surfaces cannot be resolved in the Δ spectra.[21] Obviously, the enhancement of the sensitivity achieved in the present work can be ascribed, at least in part, to the larger angle of incidence.

The relative ellipsometric data of the SAMs with varying CH_2 units are shown in Figure 6a,b. The improvements achieved by using relative optical densities are apparent from a comparison with the original ellipsometric data presented in Figure 5. There are five vibrational bands for some SAMs. It can be seen that the Fermi resonance of the symmetric CH_3 stretch r_{FR}^+ is observed near 2940 cm^{-1}, based on the KKT of the complex optical density for the four chains with C_5, C_7, C_8, and C_9. However, the r_{FR}^+ vibration becomes weaker with increasing number of CH_2 units and results in a peak with a shoulder (see the fifth arrow in Figure 6). This is ascribed to the stronger asymmetric CH_2 band, which overlaps with the r_{FR}^+ vibration and results in the shoulder structure observed for longer chains.

The vibrational frequencies of all SAMs are listed in Table 1. It should be emphasized that the data are from the original and referenced ellipsometric spectra. For the C_5 SAMs, four stretching modes originating from the CH_3 and CH_2 groups were

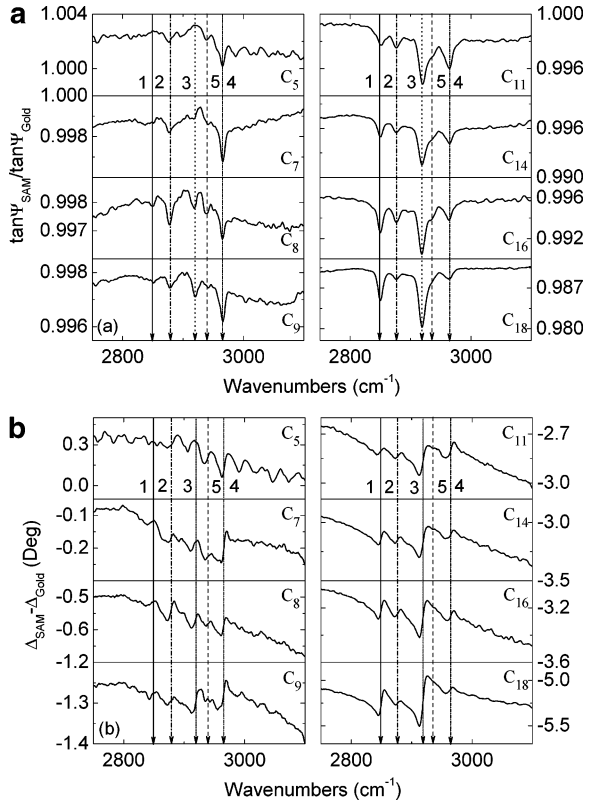

Figure 6. Relative IR ellipsometric spectra, (a) $\tan\Psi_{SAM}/\tan\Psi_{Gold}$ and (b) $\Delta_{SAM}-\Delta_{Gold}$, of C_5-C_{18} *n*-alkylthiol SAMs on gold films. For clarity, the spectra are shifted vertically; the incident angle was about 83°. Note that the absorption-like bands in part a correspond to the derivative-like patterns in part b, related by the KKT. The arrows 1, 2, 3, 4, and 5 indicate the d^+, r^+, d^-, r^-, and $r_{FR}{}^+$ C−H stretching modes, respectively, listed in Table 1.

TABLE 1: The Vibrational Frequencies of the $CH_3(CH_2)_xSH$ SAMs with Different CH_2 Units Deposited on Gold Films As Determined by IRSE (Figures 5 and 6)[a]

vibration modes	peak frequencies for $CH_3(CH_2)_xSH$ SAMs							
	C_5	C_7	C_8	C_9	C_{11}	C_{14}	C_{16}	C_{18}
d^+ (CH_2-sym)	−	−	2849	2851	2851	2850	2850	2850
r^+ (CH_3-sym)	2876	2877	2877	2877	2876	2876	2876	2876
d^- (CH_2-asym)	2927	2926	2924	2923	2922	2921	2920	2920
$r_{FR}{}^+$ (CH_3)	2940	2942	2939	2942	−	−	−	−
r^- (CH_3-asym)	2965	2966	2964	2966	2966	2964	2964	2964

[a] Note that the sensitivity of the original and relative ellipsometric spectra are different for the lower *x* values. The values are in cm^{-1}.

observed. This fact indicates that the oscillators of the CH_2 group possess a weaker strength than those of the CH_3 group, in agreement with previous results.[1] With an increasing number of CH_2 units the asymmetric CH_2 vibration d^- appears and shifts toward the lower energy side (see Figure 7). For the C_8 SAMs, the symmetric CH_2 d^+ mode can be observed, which remains fixed at 2850 cm^{-1}. This indicates that ordering by lateral interaction of SAMs improves with additional CH_2 units and further increases the d^+ and d^- oscillator strength. In addition, the strength of the asymmetric vibrations of the CH_2 and CH_3 groups becomes larger than that of the symmetric vibrations. Note that there are five well-defined vibrational modes with moderate strength for the C_8 and C_9 SAMs.

It is well-known that variation of the CH_2 units in SAMs can result in the so-called "odd−even effect", resulting in a specific behavior for an odd and even number of carbon atoms.[11,21] For SAMs containing an even number of CH_2 groups, the absorption intensity of the asymmetric CH_3 stretching

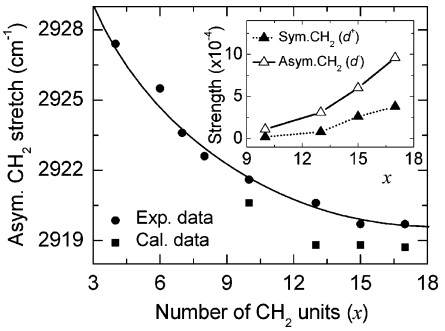

Figure 7. The variation of the asymmetric CH_2 vibration mode d^- with the number of CH_2 units of *n*-alkylthiol SAMs on gold films. "Exp." and "Cal." indicate the values taken from Tables 1 and 2, respectively. The solid line is shown to guide the eye. Note that the calculated frequencies are slightly smaller than the experimental values. The inset illustrates the increase of the signal strength with the number of CH_2 units.

vibration is higher than that of the corresponding symmetric mode, whereas the situation is reversed for SAMs containing an odd number of CH_2 groups.[21] In Figure 6, this effect is verified for various CH_2 units. When *x* is an even number (C_5, C_7, C_9, and C_{11}), there is a stronger absorption-like dip at the asymmetric CH_3 vibration position at 2962 cm^{-1} (the fourth arrow), as compared with the symmetric one at 2877 cm^{-1} (the second arrow) in the $\tan\Psi_{SAM}/\tan\Psi_{Gold}$ spectra. Correspondingly, the derivative-like band pattern shows a similar behavior in the $\Delta_{SAM}-\Delta_{Gold}$ spectra. However, the vibrational signals of SAMs containing an odd number of CH_2 groups (C_8, C_{14}, C_{16}, and C_{18}) keep the same intensity for the r^+ and r^- modes in the referenced spectra.[41] This may be due to the orthogonality of these bands and a different tilt angle of the methyl group, which is positive for an odd number of carbon atoms and negative for an even number of carbon atoms with respect to the molecular axis.[21] In addition, a different tilt angle of the chains (normally an average value of about 27° is accepted for *n*-alkylthiols normal to the gold surface), which changes with the number of CH_2 groups due to lateral interactions, can also contribute to this discrepancy.[1,11,21] Note that the average tilt angle was derived for long chains with $x \geq 15$ and the tilt angle of the shorter chains is not known.[11] It must be expected that the kinetics of SAM formation and their density and arrangement are different for shorter chains than for longer chains with stronger lateral interactions.[6]

Calculation of Spectral Data. To explain the optical response of the *n*-alkylthiol SAMs on gold films, model calculations are needed to reproduce the ellipsometric data.[16,24,38] The fitting procedure can provide accurate values for the vibrational line strength and broadening, together with the center frequency.[33,43] Owing to the effects of strong parameter correlation and undifferentiated noise, fitting becomes more difficult for short-chain SAMs.[17,18] Recently, thicknesses of 1.5 and 2.0 nm have been reported for C_{12} and C_{16} SAMs on gold films, determined by IRSE experiments.[17] Ionov et al. reproduced the $\tan\Psi$ spectra of polymer films obtained by IRSE to derive the thickness, which agreed with single-wavelength ellipsometry.[38] However, the characteristics of the vibrational line profiles were not given. In principle, SE provides access to this information with an optimized dispersion model and known substrate parameters in the ultraviolet−infrared region.[19,44] It should be noted that a simultaneous determination of the features of weak vibrational modes and the thickness of an ultrathin organic film is still an unresolved problem in optical spectroscopy.[37,45,46] The gold surface may rearrange during the formation of SAMs. This results in a change of the optical constants of the gold film−

TABLE 2: Line Parameters of Vibrational Modes of the $C_{11}-C_{18}$ SAMs As Calculated from Figure 8[a]

	d^+ (CH_2-sym)			r^+ (CH_3-sym)			d^- (CH_2-asym)			r^- (CH_3-asym)		
SAMs	S_1	$\omega_{CH,1}$	γ_1	S_2	$\omega_{CH,2}$	γ_2	S_3	$\omega_{CH,1}$	γ_3	S_4	$\omega_{CH,4}$	γ_4
C_{18}	3.8	2850	9.2	1.3	2877	12.2	9.6	2919	14.1	1.4	2963	12.7
C_{16}	2.6	2850	11.2	2.1	2877	15.0	6.0	2919	16.9	2.1	2963	18.6
C_{14}	0.8	2850	7.5	0.5	2876	9.5	3.1	2919	14.6	1.5[b]	2963[b]	20.0[b]
C_{11}	0.2	2852	7.2	0.2	2876	10.0	1.2	2921	16.0	1.3	2962	32.5

[a] The strength S_j ($\times 10^{-4}$) is dimensionless and all other parameters are in cm^{-1}. [b] The values are fixed in the calculations.

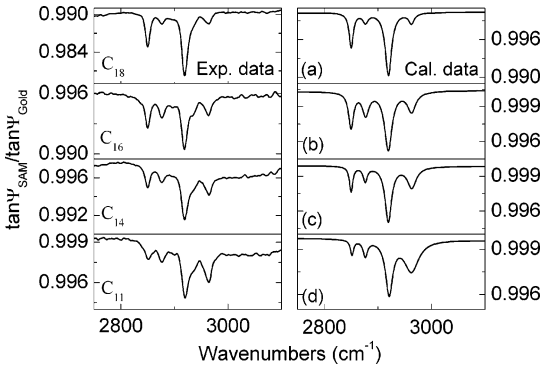

Figure 8. Comparison of the simulated real part $\tan\Psi_{SAM}/\tan\Psi_{Gold}$ for the (a) C_{18}, (b) C_{16}, (c) C_{14}, and (d) C_{11} *n*-alkylthiol SAMs on gold films with the corresponding experimental data taken from Figure 6.

substrate system in comparison with the reference spectrum applied.[17,28,47] However, this has no influence on the determination of the C−H band parameters as in Raman spectroscopy.[12,48,49]

The calculated relative ellipsometric spectra of $\tan\Psi_{SAM}/\tan\Psi_{Gold}$ of four *n*-alkylthiol SAMs (C_{11}, C_{14}, C_{16}, and C_{18}) are presented in Figure 8. Good agreement between the experimental and calculated vibrational bands is obtained. This shows that the isotropic optical model is basically suited to describe the IRSE data. The spread of the incident angle originating from the infrared beam causes deviations from the baseline[17] (i.e., $\tan\Psi_{SAM}/\tan\Psi_{Gold} = 1$ at wavenumber regions without vibration bands) which were taken into consideration in the evaluation. This produced a faster convergence in the calculations of the spectral patterns.[33,36] The deviations for longer chains (e.g., 1% for the C_{18} SAMs) may be ascribed to a nonlinear response of the detector and/or the depolarization of optical components.[30,39,50,51] The high-frequency dielectric constant ϵ_∞ was varied from 0.5 to 1.5 with increasing number of carbon atoms, whereas in the literature a constant value of 1.5 is assumed.[29,35] It must be expected that the background component varies with the symmetry and length of the alkyl chains.[29] Therefore, the above background variation seems to be plausible and does not affect the oscillator parameters of the SAMs. In addition, the thickness of the alkylthiol films was estimated. As expected, the values were in the nanometer range but not as accurate as the thicknesses determined by NIR−UV ellipsometry. As previously stated, the simultaneous determination of weak vibrations and the thickness of organic thin films is difficult in the infrared region.[18,21,52−54]

Note that the shoulder structure of the symmetric $r_{FR}{}^+$ mode near the Fermi resonance cannot be reproduced due to its weak intensity. The four stretching vibrations can be well reproduced with the Lorentz model by using the parameters listed in Table 2. The oscillator strength of the C−H stretching vibrations is in the range of $10^{-4}-10^{-5}$. For the d^+ and d^- modes of CH_2, the strength increases linearly with the number of methylene units (see the inset in Figure 7). On the other hand, there is a complicated trend for the methyl group due to the "odd−even effect". For the C_{16} and C_{18} SAMs, the strength of the r^+ and r^- modes has the same value (e.g., 1.3×10^{-4} for C_{18}), which agrees with the previous discussion. The calculated symmetric and asymmetric vibration frequencies of CH_2 shift toward the high-energy side with decreasing number of CH_2 units, with slightly smaller values than the experimental ones, as can be seen in Figure 7. This discrepancy may be due to system errors, such as the limited spectral resolution of 4 cm^{-1} and/or the mesh interval of 0.5 cm^{-1} used in the simulation. It indicates that the molecular packing density and the ordering effect of SAMs are reduced for shorter chains.[1] The broadening of the vibrational bands agrees with that reported for polymethylene chains studied by FT-IRRAS.[33,35] For example, the value of 9.2 cm^{-1} is close to the fwhm of 9.0 cm^{-1} found for the d^+ mode of the C_{18} SAM.[32] Moreover, the asymmetric vibrations are broader than the corresponding symmetric ones for the CH_2 and CH_3 groups.

4. Conclusions

In summary, IRSE spectra of C_5-C_{18} *n*-alkylthiols grown on gold films were investigated. On the basis of the optimization of the setup, it was possible to detect C−H vibrations of small chains with only five carbon atoms. There is a stronger absorption at the position of the asymmetric CH_3 vibration compared with the symmetric CH_3 vibration in the relative ellipsometric spectra of SAMs containing an even number of CH_2 groups due to the "odd−even effect". The simulated relative ellipsometric spectra provide the vibrational center frequency, the line strength, and the broadening effect. The high-frequency dielectric constant was varied from 0.5 to 1.5 with increasing number of carbon atoms. The oscillator strength of the C−H vibrations is very small and their fwhm varies between 7 and 33 cm^{-1}. It can be concluded that the IRSE technique is a very versatile tool to monitor SAMs due to its high information content, sensitivity, and nondestructivity.

Acknowledgment. One of the authors (Z.G.H.) acknowledges support from the Alexander von Humboldt Foundation. The authors thank A. Miklós, D. Lingenfelser, and N. Salingue for their technical support and many fruitful discussions.

References and Notes

(1) Li, Z. Y.; Chang, S. C.; Williams, R. S. *Langmuir* **2003**, *19*, 6744.
(2) Tour, J. M. *Acc. Chem. Res.* **2000**, *33*, 791.
(3) Reed, M. A.; Chen, J.; Rawlett, A. M.; Price, D. W.; Tour, J. M. *Appl. Phys. Lett.* **2001**, *78*, 3735.
(4) De Gennes, P. G. *Macromolecules* **1980**, *13*, 1069.
(5) Tassin, J.-F.; Siemens, R. L.; Tang, W. T.; Hadziioannou, G.; Swalen, J. D.; Smith, B. A. *J. Phys. Chem.* **1989**, *93*, 2106.
(6) Bensebaa, F.; Voicu, R.; Huron, L.; Ellis, T. H.; Kruus, E. *Langmuir* **1997**, *13*, 5335.
(7) Harrick, N. J. *Internal Reflection Spectroscopy*; Harrick Scientific Corp.: Ossining, NY, 1979.
(8) Roy, D.; Fendler, J. H. *Adv. Mater.* **2004**, *16*, 479.
(9) Hutter, E.; Assiongbon, K. A.; Fendler, J. H.; Roy, D. *J. Phys. Chem. B* **2003**, *107*, 7812.
(10) Garand, É.; Picard, J. F.; Rowntree, P. *J. Phys. Chem. B* **2004**, *108*, 8182.

(11) Laibinis, P. E.; Whitesides, G. M.; Allara, D. L.; Tao, Y.-T.; Parikh, A. N.; Nuzzo, R. G. *J. Am. Chem. Soc.* **1991**, *113*, 7152.
(12) Bryant, M. A.; Pemberton, J. E. *J. Am. Chem. Soc.* **1991**, *113*, 8284.
(13) Lummerstorfer, T.; Hoffmann, H. *Langmuir* **2004**, *20*, 6542.
(14) Azzam, R. M. A.; Bashara, N. M. *Ellipsometry and Polarized Light*; North-Holland: Amsterdam, The Netherlands, 1977.
(15) Smith, D. Y. *Handbook of Optical Constants of Solid*; Palik, E. D., Ed.; Academic: New York, 1985.
(16) Hinrichs, K.; Gensch, M.; Esser, N. *Appl. Spectrosc.* **2005**, *59*, 272A.
(17) Meuse, C. W. *Langmuir* **2000**, *16*, 9483.
(18) Bradford, D. C.; Hutter, E.; Assiongbon, K. A.; Fendler, J. H.; Roy, D. *J. Phys. Chem. B* **2004**, *108*, 17523.
(19) Tompkins, H. G.; Tiwald, T.; Bungay, C.; Hooper, A. E. *J. Phys. Chem. B* **2004**, *108*, 3777.
(20) Gensch, M.; Roodenko, K.; Hinrichs, K.; Hunger, R.; Güell, A. G.; Merson, A.; Schade, U.; Shapira, Y.; Dittrich, Th.; Rappich, J.; Esser, N. *J. Vac. Sci. Technol. B* **2005**, *23*, 1838.
(21) Bradford, D. C.; Hutter, E.; Fendler, J. H.; Roy, D. *J. Phys. Chem. B* **2005**, *109*, 20914.
(22) Greenler, R. G. *J. Chem. Phys.* **1966**, *44*, 310.
(23) Berreman, D. W. *Phys. Rev.* **1963**, *130*, 2193.
(24) Kasic, A.; Schubert, M.; Einfeldt, S.; Hommel, D.; Tiwald, T. E. *Phys. Rev. B* **2000**, *62*, 7365.
(25) Ron, H.; Rubinstein, I. *Langmuir* **1994**, *10*, 4566.
(26) Bain, C. D.; Troughton, E. B.; Tao, Y.-T.; Evall, J.; Whitesides, G. M.; Nuzzo, R. G. *J. Am. Chem. Soc.* **1989**, *111*, 321.
(27) Yang, G. H.; Amro, N. A.; Starkewolfe, Z. B.; Liu, G.-Y. *Langmuir* **2004**, *20*, 3995.
(28) Parikh, A. N.; Allara, D. L.; Azouz, I. B.; Rondelez, F. *J. Phys. Chem.* **1994**, *98*, 7577.
(29) Tillman, N.; Ulman, A.; Schildkraut, J. S.; Penner, T. L. *J. Am. Chem. Soc.* **1988**, *110*, 6136.
(30) Röseler, A.; Korte, E. H. Infrared Spectroscopic Ellipsometry. In *Handbook of Vibrational Spectroscopy*; Griffiths, P. R., Chalmers, J., Eds.; John Wiley and Sons: Chichester, UK, 2002; Vol. 2.
(31) Heaven, O. S. *Optical Properties of Thin Solid Films*; Dover: NewYork, 1991.
(32) Hu, Z. G.; Strassburg, M.; Dietz, N.; Perera, A. G. U.; Asghar, A.; Ferguson, I. T. *Phys. Rev. B* **2005**, *72*, 245326.
(33) Parikh, A. N.; Allara, D. L. *J. Chem. Phys.* **1992**, *96*, 927.
(34) Schubert, M. *Phys. Rev. B* **1996**, *53*, 4265.
(35) Hoffmann, H.; Mayer, U.; Krischanitz, A. *Langmuir* **1995**, *11*, 1304.
(36) Press, W. H.; Teukolsky, S. A.; Vetterling, W. T.; Flannery, B. P. *Numerical Recipes in C*: *The Art of Scientific Computing*; Cambridge University Press: Cambridge, MA, 1992.
(37) Palik, E. D. *Handbook of Optical Constants of Solid*; Academic: New York, 1985.
(38) Ionov, L.; Sidorenko, A.; Eichhorn, K. J.; Stamm, M.; Minko, S.; Hinrichs, K. *Langmuir* **2005**, *21*, 8711.
(39) Hinrichs, K.; Gensch, M.; Röseler, A.; Esser, N. *J. Phys.*: *Condens. Matter* **2004**, *16*, S4335.
(40) Nuzzo, R. G.; Dubois, L. H.; Allara, D. L. *J. Am. Chem. Soc.* **1990**, *112*, 558.
(41) Brunner, H.; Vallant, T.; Mayer, U.; Hoffmann, H. *Surf. Sci.* **1996**, *368*, 279.
(42) Kurth, D. G. *Langmuir* **1998**, *14*, 6987.
(43) Kuzmenko, A. B. *Rev. Sci. Instrum.* **2005**, *76*, 083108.
(44) Hilfiker, J. N.; Bungay, C. L.; Synowicki, R. A.; Tiwald, T. E.; Herzinger, C. M.; Johs, B.; Pribil, G. K.; Woollam, J. A. *J. Vac. Sci. Technol. A* **2003**, *21*, 1103.
(45) Ducharme, D.; Tessier, A.; Russev, S. C. *Langmuir* **2001**, *17*, 7529.
(46) Kattner, J.; Hoffmann, H. *J. Phys. Chem. B* **2002**, *106*, 9723.
(47) Poirier, G. E. *Chem. Rev.* **1997**, *97*, 1117.
(48) Zhang, Z. J.; Imae, T. *Langmuir* **2001**, *17*, 4564.
(49) Cardona, M. In *Resonance Phenomenon*, *Light Scattering in Solids II*; Cardona, M., Güntherodt, G., Eds.; Springer: Berlin, Germany, 1982.
(50) Zhang, Z. M.; Zhu, C. J.; Hanssen, L. M. *Appl. Spectrosc.* **1997**, *51*, 576.
(51) Canillas, A.; Pascual, E.; Drévillon, B. *Rev. Sci. Instrum.* **1993**, *64*, 2153.
(52) Buffeteau, T.; Desbat, B.; Turlet, J. M. *Appl. Spectrosc.* **1991**, *45*, 380.
(53) Allara, D. L.; Baca, A.; Pryde, C. A. *Macromolecules* **1978**, *11*, 1215.
(54) Kurth, D. G.; Bein, T. *Langmuir* **1995**, *11*, 578.